SMiRT–12 / K. Kussmaul (Editor)
© 1993 Elsevier Science Publishers B.V. All rights reserved.

C05/4

LATERAL COMPRESSION STRENGTH OF GRAPHITE FUEL ELEMENTS

F.H. Ho

General Atomics, P.O. Box 85608, San Diego, CA 92186, USA

SUMMARY

Static lateral compression tests were performed on prismatic graphite fuel element sections. Load deflection curves obtained are essentially linear. The stiffness of the standard element is 1.08 MN/mn and is in excellent agreement with finite element analysis results. The mean ultimate compression strength of the standard fuel element is 787 kN.

Fracture patterns are usually reproducible. Cracks at the edge of the loaded area are the first to propagate to final failure. The initial cracking load in the test specimen can be determined by the sudden change in the acoustic emission count data obtained through microphonics. The initial cracking load is much closer to the analytical prediction than the ultimate load.

1. INTRODUCTION

Prismatic standard fuel elements made of H-451 graphite are used in the core of the U.S. designed Modular Helium Reactor (MHR) as moderator and structural components. These graphite core elements are subjected to lateral impact loadings in a seismic event, in addition to thermal and irradiation-induced loads. The lateral seismic strength of standard fuel elements is needed in order to evaluate its structural integrity in a seismic event.

In the past, linear elastic finite element stress analyses were performed on graphite structures to evaluate their strength. Comparison with experimental data showed that the data are always higher than the analytical predictions by a factor as high as two. The maximum principal stress theory was used in the analyses, and the ultimate tensile strength was always taken as the failure stress. Because of the inability of the analysis to predicting failure, lateral strength of fuel elements cannot be reasonably estimated with high confidence by analysis alone. Hence, a test program with emphasis on standard elements was proposed. This paper documents the experimental methods, results and findings of the test program.

2. TEST SPECIMENS

Three standard fuel elements were purchased form Great Lakes Carbon Company for testing. All the elements are a hexagonal prism with an axial height of ~79 cm. Their configuration is shown in Fig. 1.

The elements were machined into three equal sections along the axial direction. These three sections are not identical in detailed geometry. The top section has three shallow dowel holes at the upper end and a fuel handling hole at the center that goes all the way through the test section.

The middle section has only a portion of the fuel handling hole at the center. The depth of the hole is approximately equal to one half of the section length. The bottom section has three slightly elongated dowel holes and a center tooling hole at the lower end. In addition to these, all fuel holes are blind.

All element sections are designated by a letter T or M or B, following the log number to represent either top, middle or bottom one-third of a fuel element, respectively.

In analysis of test data later, the detailed differences in the sectional geometry will not be considered. The ultimate load and stiffness of a fuel element is assumed to be equal to the sum of the ultimate loads and the stiffness of its three element sections.

3. EXPERIMENTAL METHODS

Flat face static compression tests were made on all 12 element sections. All testing was done in a standard 26.7 kN Baldwin Universal test machine. The loading rate was controlled at about 1 kN/s. Load deflection curve was recorded for each specimen and test machine itself. The deflection was the relative displacement between the lower grip plate and the quarter point of the cross-head beam.

A transducer was attached to the slanted top surface of the specimen prior to the start of the testing. Acoustic signals with intensity of 90 db or higher were counted, accumulated, and recorded continuously on a chart.

Most of the specimens were tested monotonically to failure. A few specimens were either held at a constant load for a short period of time or unloaded and them reloaded once or twice. Two specimens did not fail at the maximum capacity of the test machine and were being held at the maximum load and unload when either the acoustic noises faded away (crack arrest) or a continuous cracking was observed. A photo was taken for every specimen after the test.

4. RESULTS AND DISCUSSION

The load deflection curves of specimen sections recorded include the effect of the test machine compliance. The results presented below have been modified to remove the test machine compliance from the load-deflection curve.

Ultimate load (P_u), maximum deflection (δ_m), stiffness at 89 kN (the maximum expected seismic load) for every individual section and the whole fuel element are given in Table 1. The average ultimate load of a standard element is 787 kN. The bottom section, where the fuel holes are blind, has an ultimate load consistently more than 10% higher than that of the top middle sections. Sections 3B and 2B did not fail at 267 kN, the maximum capacity of the machine. The failure loads for these two sections in Table 1 were estimated from the acoustic emission counts, as will be explained later. The ultimate load obtained here is equal to 1.7 times the finite element analysis result.

Almost linear load deflection curves of graphite components are not solely a characteristic of the present test. Early tests on fuel elements [1] showed a linear monotonic load deflection curves. slight nonlinearity was gradually introduced when unloading and reloading at medium or high load levels occurred. The degree of nonlinearity is also less than that of a uniaxial tensile or bend specimen under a monotonic load. It is not yet fully understood or demonstrated why the aggregate of nonlinear elements exhibits less degree of nonlinearity. Perhaps a major portion of material volume is still at low stress level. Cracking at the peak stress locations cause redistribution of stress.

The fracture pattern falls into two categories. The first pattern was the splitting of an element section diagonally into two equal segments that are trapezoidal in shape. The initial extensive cracking that resulted in catastrophic failure presumably started at or beyond the edge of the loaded area. When the load increased continuously, local cracks occurred at the top or the bottom of the fuel and cooling holes along the diagonal crack path, and eventually propagated and connected to yield the fracture pattern. All the top sections failed this way. This mode of failure has been observed in the early test and reported in [1].

The fuel element in the second pattern broke into three or four main segments. Normally a triangular section under the loaded was pushed into the specimen to split it into three pieces.

Although macro-cracks were observed at many locations below or near the ultimate load, the crack front that propagated into physical separation of the element section is believed to have started at the edge of the loaded area. This is supported by a specimen (3B) which was loaded to ~93% of the ultimate load, and then unloaded. The extensive cracking pattern clearly indicated that failure started at the loaded edge.

Acoustic emission data, including acoustic and cumulative counts, indicated that some isolated noises were generated even at low load level. These are presumably due to cracking of some constraining "tight" ligaments in a porous graphite component. The cumulative count is still small. When the load increased to a certain level, the density of the acoustic count increased rapidly, indicating the start of intensive cracking. The cumulative count at this load level is usually between 5000 to 30,000 with an average of 13,000. P_i is given in Table 2. P_i is about 70% of the ultimate load, P_u. The load deflection curve was still linear.

Beyond P_i the cumulative count increased exponentially. The envelope of the recording plot of the acoustic count is bell-shaped due to the inability of the mechanical pen to respond to the incoming signals. This bell-shaped portion of the traces are all alike for the test specimens. It spans a load increment of approximately 30% of P_u. This was the basis used to estimate the ultimate loads of the two specimens, 3B and 2B.

Specimens 3T and M were held at 89 kN for several minutes, absolutely no cracking noise was heard. Specimen 1B was stopped at 189 kN for 20 sec, no acoustic signal was recorded. This indicates crack arrest. No additional deflection was observed.

Specimen 2B was first loaded to 89 kN and unloaded. During reloading the specimen was very quiet until past 89 kN load. This was also the case for 15034T and M. Specimen 2B was continuously loaded to 267 kN and unloaded and reloaded two times. During reloading a few isolated noises were recorded when the load was near and reaching 267 kN. The specimen was held at that load point. Continuous cracking sounds were still heard, but the intensity and number of counts decreased in time. It was unloaded until the sound was almost died out. The specimen showed no visible crack. Arrest of micro-cracks was implied. The ultimate load was estimated by the acoustic count traces to be 297 kN. The load with crack arrest is close to 90% of the ultimate load.

Another specimen 3B was tested similar to the specimen 2B. The cracking sound was heard continuously when it was held at a constant load of 267 kN, which is equivalent to 93% of the estimated ultimate load of 287 kN. The noise increased in intensity and density with time. Cracks were extensive in the specimen and the test was stopped prior to physical separation of the specimen. The crack pattern clearly indicated that the running crack front started at the edge of the loaded area.

It appears that a load criterion that separates the crack arrest and the crack propagation is about 90 to 93% of the ultimate load. This is in good agreement with the static fatigue test data of Wilkins [2].

Acoustic emission data and fracture pattern are instructive in locating sources of inelastic response. It is primarily related to interlayer crack formation in the crystallites. Increasing stress generates extensive macro-cracking parallel to the layering direction in the grains and/or along the grain boundary. Constitutive relations modeling the graphite should consider the difference in mechanism as compared to metal whose plastic behavior is due to slip in the basal plane. In the latter, the maximum shear stress criterion and the classical plasticity theory apply.

The maximum tensile stress criterion was adopted in the analysis. If 1.7 times UTS is used (1.7 = the ratio of flexural strength to UTS for H-451), the ultimate load ratio of the test data to the analysis result is 1.0, instead of 1.7 as previously reported for the standard elements.

5. CONCLUSIONS

(1) Load-deflection curves of the graphite fuel elements under flat face lateral compression were essentially linear, although uniaxial tensile stress strain curves usually showed some degree of nonlinearity.

(2) Stiffness of the standard fuel elements are 1.08 MN/mm and are in excellent agreement with the finite element analysis results.

(3) Ultimate static compressive strengths are 787 kN for the standard fuel element. This strength

is about 70% higher than the corresponding finite element analysis result which used the ultimate tensile strength (UTS) as the failure stress.

(4) Cracks at the edges of the loading plates are believed to propagate first and connect macro-cracks in the interior of the element while in route to disintegration of the test element. Two fracture patterns were observed, either the block was split diagonally into two large pieces or the triangular piece under the loading plates were forced to split the block vertically into three or four large pieces.

(5) Acoustic emission data apparently defined a point of initial intensive cracking. The cumulative acoustic count at this point is approximately the same for all specimens.

(6) The static fatigue strength that separates the crack arrest and crack propagation is at about 90 to 93% of the ultimate load.

6. REFERENCES

[1] Sevier, L., "LHTGR Graphite Fuel Element Seismic Strength," GA-A13920, General Atomics, San Diego, CA, April 1976.

[2] Wilkins, B. J. S., "Static Fatigue of Graphite, " J. Am. Cera. Soc., V.54 No. 12, December 1971.

Table 1. Summary of test results for H451 standard fuel elements

Element or Section I.D.	P_u, Ultimate Load, kN	σ_m, Max. Deflection, mm	Stiffness at 89 kN, MN/mm
1T	256.	0.897	0.322
1M	241.	0.777	0.327
1B	260.	0.701	0.396
1	757.		1.045
2T	260.	0.785	0.363
2M	265.	0.841	0.350
2B	297.	0.836	0.382
2	822		1.095
3T	246.	0.810	0.331
3M	250.	0.848	0.347
3B	287.	0.790	0.434
3	783.		1.112

Table 2. Initial cracking loads and cumulative acoustic counts for standard fuel elements

Section I. D.	P_i, Initial Cracking Load, kN	Cumulative Acoustic Counts @ P_i, 10^4	Cumulative Acoustic Counts @ P_u, 10^6
1T	187.	3	~1
1M	166.	1.4	1
1B	144.	~1	~1
2T	182.	1.3	1
2M	178.	~1.5	1
2B	196.	2.5	-
3T	166.	1	~1
3M	215.	0.5	~1
3B	218.	~1	-

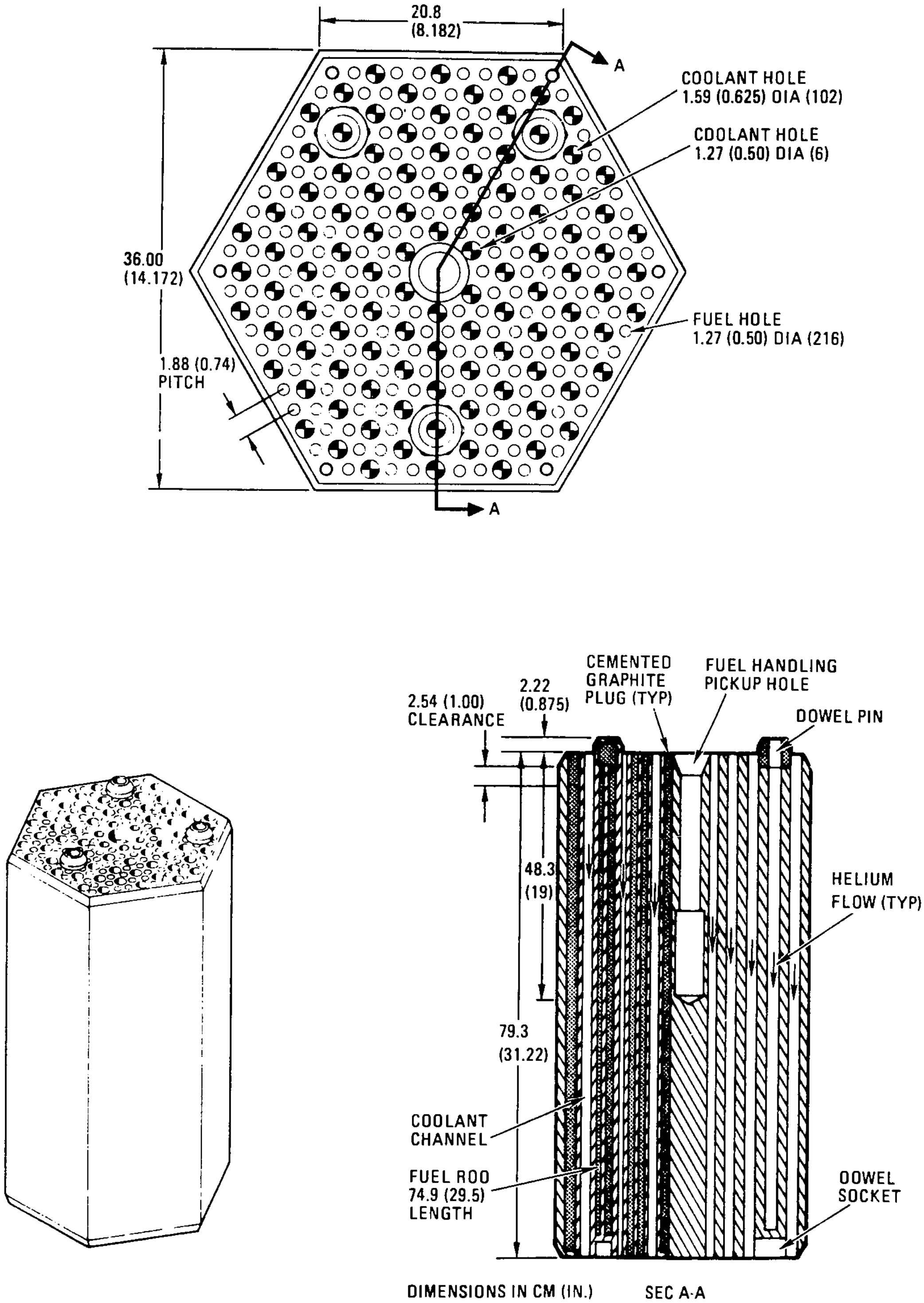

Fig. 1. STANDARD FUEL ELEMENT